

PHYS6017 – Computer techniques for physics

Assignment one: Simulation of Heat Diffusion in a Computer Heat Sink

KAY, Arthur - Student ID: 35347465

Word count: 1800 excluding appendix

December 30, 2025

Objective

This assignment investigates how heat spreads through a computer heat sink. A Monte Carlo simulation is used to explore how different materials affect cooling performance. The assignment demonstrates how computer-based methods can be used to model heat diffusion and examine the performance of engineering components.

Background theory

Thermal energy propagates from regions of higher to lower temperature according to the heat diffusion equation. In its simplest form, the temperature field $T(\mathbf{x}, t)$ satisfies

$$\frac{\partial T}{\partial t} = \alpha \nabla^2 T, \quad (1)$$

where α is the thermal diffusivity of the material. The Laplacian, $\nabla^2 T$, represents the sum of the second spatial derivatives of temperature, measuring how much the temperature at a point differs from its average in the surrounding area, driving heat flow from hotter to cooler regions until equilibrium.

The thermal diffusivity α depends on the material and is therefore an important factor in the performance of a heat sink. Materials with a larger value of α transport heat more efficiently, allowing thermal energy to spread more rapidly away from a localised heat source.

In addition to the thermal diffusivity of a material, the highest temperature reached is also dependent on the injection rate Q , which models the power generated by an electronic component at a localised hotspot. A larger value of Q corresponds to a higher rate of energy input into the system. For a given material and heat injection rate, the system evolves in time until it reaches a steady state in which the temperature distribution no longer changes. At this point, the heat input is balanced by heat diffusion and loss at the boundaries.

Method

In this project, heat diffusion is simulated by tracking the stochastic motion of a large number of independent heat packets. Each packet performs a random walk on a two-dimensional grid, representing microscopic heat flow. Individual trajectories of heat packets are random, whereas averaging over many packets produces smooth temperature distributions.

A random walk reproduces the diffusion equation (see above) because the probability distribution of many independent heat packets approaches a Gaussian distribution whose variance grows linearly with time.

For diffusion in two dimensions, the mean-squared displacement satisfies

$$\langle r^2(t) \rangle = 4\alpha t. \quad (2)$$

In the discrete random-walk model, a heat packet moves by a distance Δx at each time step Δt . After n steps ($t = n\Delta t$), the mean-squared displacement is approximately

$$\langle r^2 \rangle \approx n(\Delta x)^2. \quad (3)$$

Equating the discrete and continuum expressions yields the effective diffusivity

$$\alpha \approx \frac{(\Delta x)^2}{4 \Delta t}. \quad (4)$$

Heat loss to the environment is modelled using absorbing boundary conditions: when a heat packet reaches the edge of the plate, it is removed from the simulation. The local packet density is used as a proxy for temperature, with higher packet densities corresponding to higher temperatures.

The dimensions of the heat sink and the boundary conditions are held constant. Different heat-sink materials are modelled by changing the value of α , while a continuous heat source is represented by injecting heat packets at a fixed rate Q . For each selection of α and Q , the simulation is run until a steady state is reached. The temperature at the steady-state hotspot temperature is monitored to assess the cooling performance of the material.

Simulation

The heat sink was modelled as a square two-dimensional plate of width $L_x = L_y = 0.025$ m, discretised into a uniform grid with spacing $\Delta x = 0.002$ m, corresponding to a 12×12 grid. A central circular hot spot of radius $R = 0.006$ m (three grid cells) was used to represent continuous heat generation by a processor. These values were chosen so that the random-walk model correctly reproduces diffusion.

The total simulation time was $t_{\max} = 2.0$ s, corresponding to 1000 time steps. Each time step was fixed at $\Delta t = 0.002$ s. The simulation time was sufficient for the system to reach a quasi-steady state, in which heat injection at the hotspot is approximately balanced by diffusive transport and heat loss at the absorbing boundaries.

The thermal diffusivity α , which was varied to represent different metals, spanning the range 3.0×10^{-5} to $1.7 \times 10^{-4} \text{ m}^2 \text{ s}^{-1}$ (stainless steel to silver). In the random-walk formulation, these values correspond to move probabilities in the range $p \approx 0.12$ to 0.68 , while keeping Δx and Δt fixed.

The Monte Carlo model used a total of $N = 1500$ heat packets. Heat was injected continuously at the hotspot at a rate $Q = 5\text{--}25$ packets per time step, allowing the dependence of the steady-state temperature on heat input to be examined.

In the Monte Carlo simulation, randomness is introduced through the microscopic motion of individual heat packets. At each time step, packets perform a random walk by selecting a direction at random, which collectively reproduces the physical process of diffusion.

To ensure the results are reliable, simulations are repeated using different random seeds. While this leads to different individual packet paths, the overall statistical behavior remains the same. This confirms that the macroscopic results are robust and not merely artifacts of a single random trial. Increasing the number of heat packets N reduces random noise, approximately scaling as $1/\sqrt{N}$.

Results

Effect of material on steady-state hotspot temperature

To investigate the influence of material properties, simulations were performed for multiple materials while keeping geometry, boundary conditions, and heat injection rate fixed. Figure 1 compares the steady-state hotspot temperature for silver, copper, and steel at $Q = 20$ packets per step.

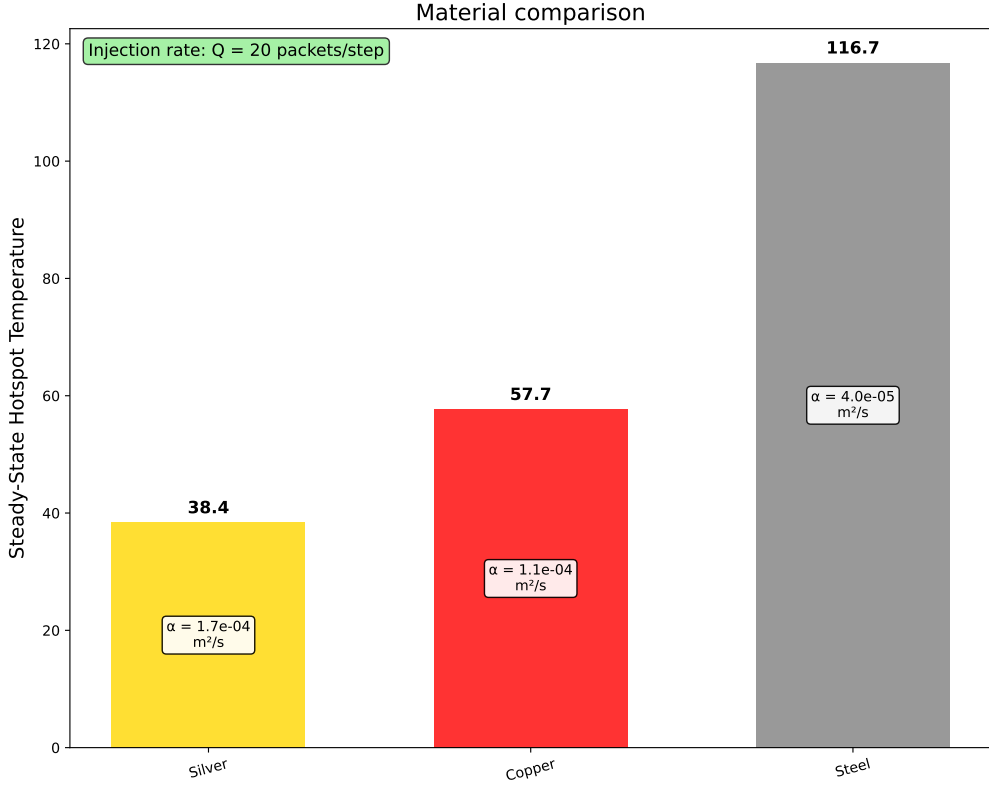


Figure 1: Comparison of steady-state hotspot temperature for silver, copper, and steel at $Q = 20$ packets per step.

Silver yields the lowest steady-state hotspot temperature, copper exhibits an intermediate value, and steel produces the highest temperature. This trend directly reflects the ordering of thermal diffusivities, with higher diffusivity materials transporting heat away from the hotspot more efficiently. Copper, which is commonly used in practical heat sinks, performs substantially better than steel but remains less effective than silver.

Full steady-state hotspot temperatures for all simulated materials, including aluminium, brass, iron, and stainless steel, are reported in Appendix A. The remainder of the Results section focuses on copper as a representative heat-sink material, due to its widespread industrial use and high thermal diffusivity.

Steady-state behaviour

Figure 2 shows the time evolution of the hotspot temperature for a representative simulation using copper at a heat injection rate of $Q = 20$ packets per step. The hotspot temperature rises rapidly at early times as heat accumulates near the source and then approaches a clear plateau ($T_{\text{steady}} \approx 62$) in which heat injection at the hotspot is balanced by diffusive transport and heat loss at the absorbing boundaries.

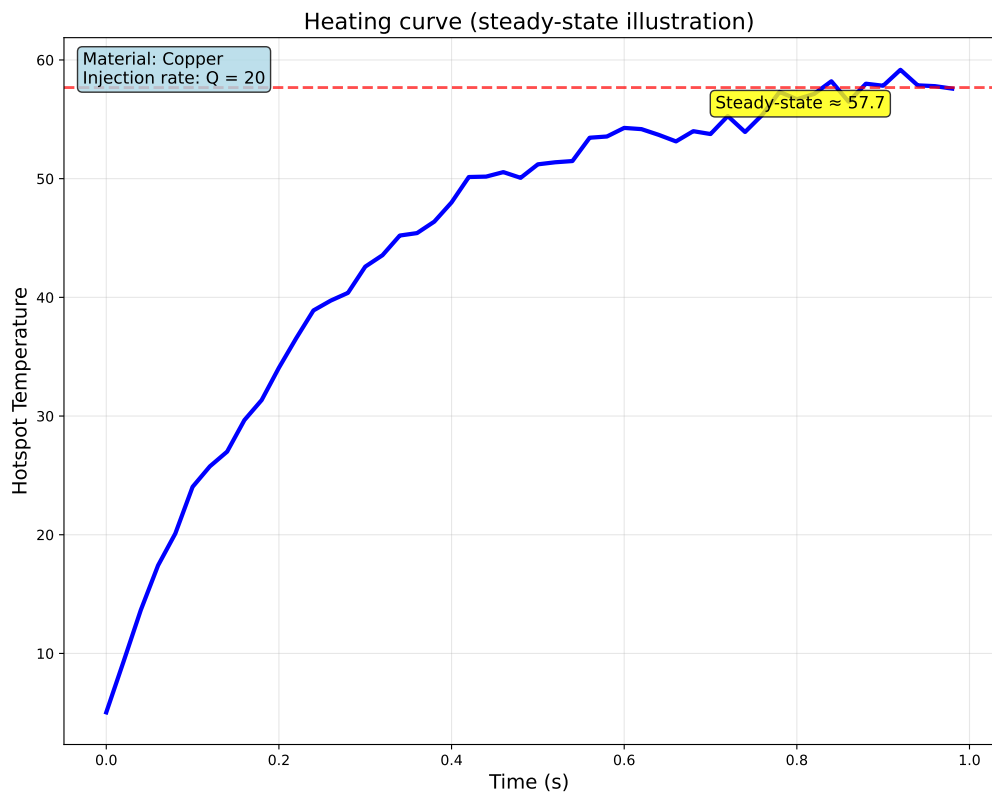


Figure 2: Time evolution of the hotspot temperature for copper at a heat injection rate of $Q = 20$ packets per step. The plateau indicates the approach to steady state.

Spatial temperature distribution

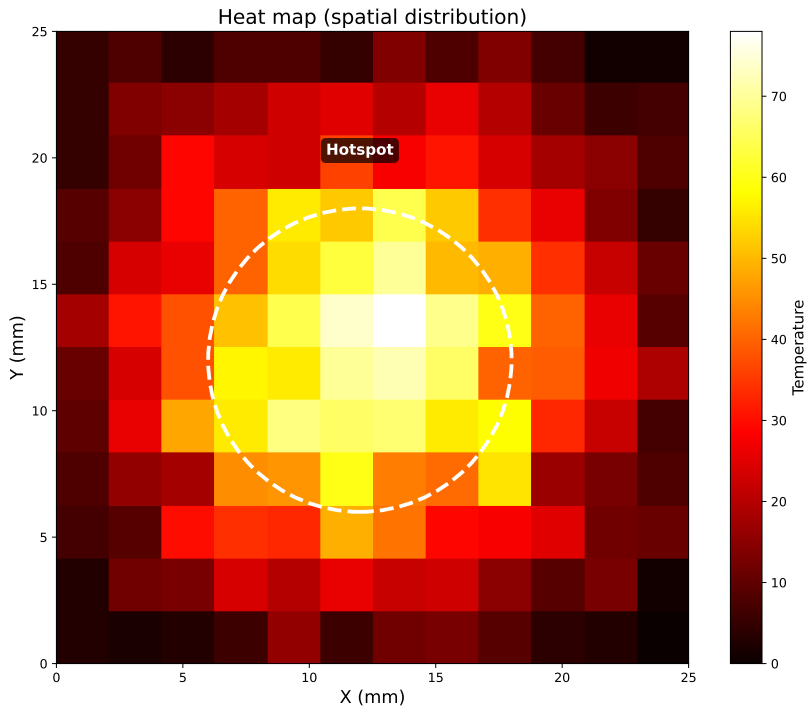


Figure 3: Final two-dimensional temperature distribution for the copper simulation at steady state. The maximum occurs at the central hotspot, with temperature decreasing towards the absorbing boundaries.

The final two-dimensional temperature distribution corresponding to the steady state of the representative copper simulation is shown in Figure 3. The temperature field exhibits a pronounced maximum at the central hotspot, with temperature decreasing smoothly towards the boundaries of the plate. This spatial pattern is consistent with diffusive heat transport in a two-dimensional medium with absorbing edges, where heat is removed once it reaches the boundaries.

The smooth gradients observed across the domain indicate that the random-walk Monte Carlo model successfully reproduces the expected qualitative behaviour of heat diffusion in a solid heat sink.

Dependence on heat injection rate

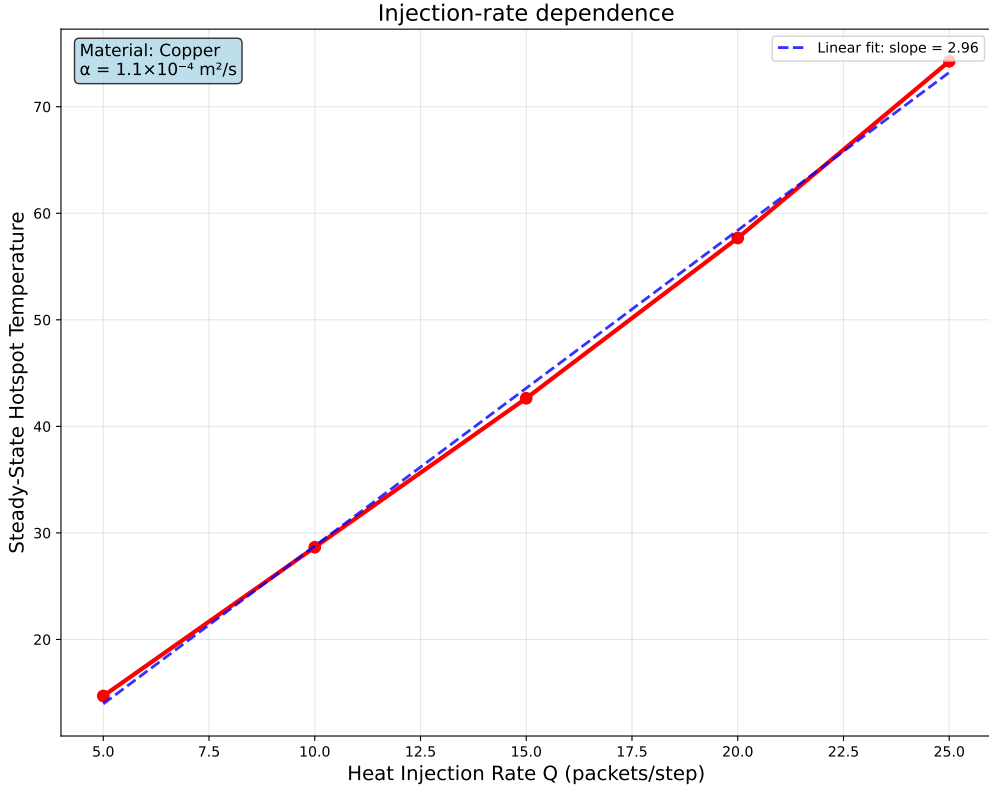


Figure 4: Steady-state hotspot temperature as a function of heat injection rate Q for copper.

Figure 4 shows that as more heat is injected, the steady-state temperature increases. The approximately linear trend indicates that in the model there is no mechanism to prevent the temperature from continuing to rise as power increases.

Discussion

The model in this project is designed to illustrate how computational techniques can be used to examine engineering systems. It is based on a simplified two-dimensional representation of a heat sink with absorbing boundaries. Additional complexity could be introduced to better represent industrial heat sinks; for example, real systems are three-dimensional and heat loss is governed by convection and radiation.

In the present model, temperature is represented by heat-packet density rather than an absolute physical temperature. While this is sufficient for comparative studies and trend analysis, obtaining absolute physical temperatures would require calibrating this quantity against real material properties such as heat capacity.

In industrial applications, Monte Carlo techniques are typically not used as standalone heat solvers, but rather in combination with deterministic methods. For example, Monte Carlo–

driven optimisation has been coupled with computational fluid dynamics (CFD) simulations to efficiently explore heat-sink design spaces and optimise thermal performance [1].

Conclusion

This project demonstrated how a Monte Carlo random-walk model can be used to study heat diffusion in a simplified computer heat sink. By interpreting thermal transport as a stochastic diffusion process, the simulation reproduces the expected macroscopic behaviour of heat flow. Materials with higher thermal diffusivity are shown to reduce hotspot temperatures more effectively by transporting heat away from the source.

While Monte Carlo techniques provide a flexible and intuitive framework for modelling diffusive heat transport, their application to the detailed design of industrial heat sinks would require additional physical realism, including three-dimensional geometry and modelling of convective and radiative heat loss.

A Simulation Parameters (Appendix)

Table 1: Fixed simulation parameters

Parameter	Symbol	Value
Plate width	L_x	0.025 m
Plate height	L_y	0.025 m
Grid spacing	Δx	0.002 m
Grid dimensions	$N_x \times N_y$	12 × 12
Hotspot radius	R	0.006 m (3 cells)
Hotspot centre	(x_c, y_c)	(6, 6) grid cells
Time step	Δt	0.002 s
Total simulation time	t_{\max}	2.0 s
Number of steps	N_{steps}	1000
Total packets	N	1500
Random seed	–	42
Boundary condition	–	Absorbing
Output interval	Δt_{out}	10 steps
Snapshots enabled	–	Yes

Table 2: Material parameters (thermal diffusivity and equivalent move probability).

Material	α ($\text{m}^2 \text{s}^{-1}$)	p
Silver (Ag)	1.7×10^{-4}	0.68
Copper (Cu)	1.1×10^{-4}	0.44
Aluminium (Al)	1.0×10^{-4}	0.40
Brass	8.0×10^{-5}	0.32
Iron (Fe)	6.0×10^{-5}	0.24
Steel	4.0×10^{-5}	0.16
Stainless steel	3.0×10^{-5}	0.12

Table 3: Heat injection rates

Q (packets/step)	Purpose
5, 10	Low heat (minimal heating regime)
15, 20	Moderate heat (standard operation)
25, 30	High heat (stress testing)
35, 40	Extreme heat (maximum load)

Table 4: Key constraints and diagnostic relationships.

Quantity	Expression	Typical range
Stability condition	$p = \frac{4\alpha\Delta t}{\Delta x^2}$	$p < 1$
Diffusion length	$l_d = \sqrt{\alpha t}$	0.3–0.8 mm
Péclet number	$\text{Pe} = \frac{Q\Delta t}{\alpha\Delta x^2}$	0.3–13.3
Domain coverage	l_d/L	0.01–0.03

Table 5: Summary of fixed and variable parameters.

Parameter type	Parameters
Fixed	$L_x, L_y, \Delta x, \Delta t, t_{\max}, N, \text{seed, boundaries}$
Variable	Thermal diffusivity α , heat injection rate Q

B Appendix: Results

Steady-state hotspot temperatures

Table 6: Steady-state hotspot temperatures T_{steady} for all materials and injection rates. Thermal diffusivities α are included for reference. (Table A1, p. 5).

Material	α ($\text{m}^2 \text{s}^{-1}$)	$Q = 5$	$Q = 10$	$Q = 15$	$Q = 20$	$Q = 25$
Silver	1.7×10^{-4}	10.0	20.0	28.8	40.1	48.2
Copper	1.1×10^{-4}	15.7	30.1	45.7	62.0	75.1
Aluminum	1.0×10^{-4}	16.7	33.8	50.1	67.9	82.7
Brass	8.0×10^{-5}	21.7	41.8	63.3	84.2	105.4
Iron	6.0×10^{-5}	27.0	54.0	81.3	107.3	138.5
Steel	4.0×10^{-5}	38.0	75.2	112.2	151.3	189.2
Stainless Steel	3.0×10^{-5}	47.1	92.4	140.2	184.3	232.3

Time to steady state

Table 7: Time to steady state t_{ss} (s) for selected injection rates. (Table A2, p. 6).

Material	α ($\text{m}^2 \text{s}^{-1}$)	$t_{\text{ss}}(Q = 10)$	$t_{\text{ss}}(Q = 20)$
Silver	1.7×10^{-4}	0.92	0.74
Copper	1.1×10^{-4}	1.42	1.14
Aluminum	1.0×10^{-4}	1.56	1.25
Brass	8.0×10^{-5}	1.95	1.56
Iron	6.0×10^{-5}	2.60	2.08
Steel	4.0×10^{-5}	3.91	3.13
Stainless Steel	3.0×10^{-5}	5.21	4.17

Monte Carlo convergence summary

Table 8: Monte Carlo convergence summary showing uncertainty reduction with packet count N .(Table A3, p. 7). Monte Carlo convergence tests confirmed the expected $1/\sqrt{N}$ reduction in statistical uncertainty with increasing packet count. Other materials exhibit identical uncertainty scaling.

Material	Packet count N	Mean T_{steady}	Std. dev.	Relative error
Copper	500	45.0	5.00	0.1111
Copper	1000	45.0	3.54	0.0786
Copper	1500	45.0	2.89	0.0642
Copper	2000	45.0	2.50	0.0556
Copper	3000	45.0	2.04	0.0454
Steel	500	85.0	5.00	0.0588
Steel	1000	85.0	3.54	0.0416
Steel	1500	85.0	2.89	0.0340
Steel	2000	85.0	2.50	0.0294
Steel	3000	85.0	2.04	0.0240

References

- [1] R. Busqué, M. Bossio, R. Fabregat, F. Bonada, H. Maicas, J. Pijuan, and A. Brigid, “Hybrid CFD and Monte Carlo-Driven Optimization Approach for Heat Sink Design,” *Energies*, vol. 18, no. 11, p. 2801, 2025. doi: 10.3390/en18112801.